Molecular Pharmacology Fast Forward. Published on September 4, 2007 as doi:10.1124/mol.107.035980
This article has not been copyedited and formatted. The final version may differ from this version.

Title page

Evidence for functional $P2X_4$ / $P2X_7$ heteromeric receptors

Chang Guo, Marianela Masin, Omar S. Qureshi, Ruth D. Murrell-Lagnado

Department of Pharmacology, University of Cambridge, Tennis Court Road, Cambridge CB2 1PD, United Kingdom

Molecular Pharmacology Fast Forward. Published on September 4, 2007 as DOI: 10.1124/mol.107.035980
This article has not been copyedited and formatted. The final version may differ from this version.

Running title page

$P2X_{4/7}$ heteromeric receptors

Corresponding author: ***Dr. Ruth Murrell-Lagnado, Department of Pharmacology, University of Cambridge, Tennis Court Road, Cambridge CB2 1PD, United Kingdom.***

E-mail: rdm1003@cam.ac.uk.

Tel: 44-1223-334011

Fax: 44-1223-334040

Number of text pages: ***29***

Number of tables: 0

Number of figures: 6 + 2

Number of references: 36

Number of words in Abstract: 245

Number of words in Introduction: 458

Number of words in Discussion: 855

Abbreviations:; BzATP, 2',3'-O-(benzoyl-4-benzoyl)-ATP; DMEM, Dulbecco's modified Eagle's medium; EGFP, enhanced green fluorescent protein; ER, endoplasmic reticulum; FITC, fluorescein isothiocyanate; HA, hemagglutinin; HEK, human embryonic kidney; NRK, normal rat kidney; BMDM, bone marrow derived macrophages; PBS, phosphate-buffered saline; SDS-PAGE, sodium dodecylsulfate-

polyacrylamide gel electrophoresis; TNP-ATP, 2',3'-O-(2,4,6-trinitrophenyl) adenosine 5-triphosphate; BBG, Brilliant Blue G; EC, extracellular; wt, wild type.

Molecular Pharmacology Fast Forward. Published on September 4, 2007 as DOI: 10.1124/mol.107.035980
This article has not been copyedited and formatted. The final version may differ from this version.

Abstract

The cytolytic ionotropic ATP receptor, $P2X_7$, has several important roles in immune cell regulation such as cytokine release, apoptosis and microbial killing. Although $P2X_7$ receptors are frequently co-expressed with another subtype of P2X receptor, $P2X_4$, they are thought not to form heteromeric assemblies but to function only as homomers. Both receptors play a role in neuropathic pain and therefore understanding how they co-ordinate the cellular response to ATP is important for the development of effective pain therapies. Here we provide biochemical and electrophysiological evidence for an association between $P2X_4$ and $P2X_7$ that increases the diversity of receptor currents mediated via these two subtypes. The heterologously expressed receptors were co-immunoprecipitated from HEK293 cells, and the endogenous $P2X_4$ and $P2X_7$ receptors were similarly co-immunoprecipitated from bone marrow derived macrophages. In HEK293 cells the fraction of $P2X_4$ receptors biotinylated at the plasma membrane increased 2-fold in the presence of $P2X_7$ although there was no change in overall expression. Co-expression of a dominant negative $P2X_4$ mutant (C353W) with $P2X_7$, inhibited $P2X_7$-receptor mediated currents by greater than 2 fold, whereas a non-functional but non-dominant negative mutant (S341W) did not. Co-expression of $P2X_4$S341W with $P2X_7$ produced a current that was potentiated by ivermectin (IVM) and inhibited by 2',3'-O-(2,4,6-trinitrophenyl) adenosine 5-triphosphate (TNP-ATP), whereas expression of $P2X_7$ alone produced a current that was insensitive to both these compounds at the concentrations used. These results demonstrate a structural and functional interaction between $P2X_4$ and $P2X_7$ which suggests that they associate to form heteromeric receptors.

Molecular Pharmacology Fast Forward. Published on September 4, 2007 as DOI: 10.1124/mol.107.035980
This article has not been copyedited and formatted. The final version may differ from this version.

Introduction

Extracellular ATP acts as a signalling molecule exerting effects on a range of biological functions including immune regulation, apoptosis, cellular proliferation and neurotransmission (Khakh and North, 2006). P2X receptors are cationic channels gated by extracellular ATP of which seven subtypes have been identified which assemble either as homo- or hetero-trimeric receptors (Barrera et al., 2005; North, 2002). Heteromerisation can change both the functional and pharmacological properties of P2X receptors (King et al., 2000; Lewis et al., 1995). One member of this family, $P2X_7$ receptor is thought to be unique amongst P2X receptors in only forming homomeric assemblies (Torres et al., 1999).

Activation of $P2X_7$ receptors, which are expressed in a range of immune cells, can result in release of Il-1β, Il-18, tumor necrosis factor -α (TNF-α) and matrix metalloproteinase 9, activation of the stress-activated protein kinase/JNK pathway, membrane blebbing and apoptotic or necrotic cell death (Gu and Wiley, 2006; Humphreys et al., 2000; Perregaux et al., 2000; Wilson et al., 2002). This receptor represents an important target in inflammatory diseases such as arthritis, neuropathic pain and stroke (Chessell et al., 2005; Dell'Antonio et al., 2002; Labasi et al., 2002). In immune cells such as macrophages, monocytes, and microglia, $P2X_7$ receptors are co-expressed with another member of the P2X family also important in neuropathic pain, the $P2X_4$ receptor (Bowler et al., 2003; Xiang and Burnstock, 2005). The role of this receptor in immune cells is not as well understood, however it has considerably higher affinity for ATP than the $P2X_7$

Molecular Pharmacology Fast Forward. Published on September 4, 2007 as DOI: 10.1124/mol.107.035980
This article has not been copyedited and formatted. The final version may differ from this version.

receptor and its up-regulation in spinal cord microglia as a result of peripheral nerve injury contributes to allodynia type hypersensitivity (Tsuda et al., 2003).

Co-expression of $P2X_4$ and $P2X_7$ is not restricted to immune cells. They are also present together in endothelial and epithelial cells and a recent, electrophysiological study of P2X receptors that are present in ciliated airway epithelia and thought to be important for mucociliary clearance, reported currents with a novel combination of both $P2X_7$ and $P2X_4$ receptor characteristics (Ma et al., 2006). Comparing amino acid sequences, $P2X_4$ is more homologous to $P2X_7$ (~40%) than are the other P2X receptor subtypes, however a previous co-immunoprecipitation study with heterologously expressed receptors failed to provide evidence for the formation of stable $P2X_{4/7}$ complexes (Torres et al., 1999).

To understand how receptors transmit an ATP signal we need to define the subunit identity of the physiological receptors. The formation of a $P2X_{4/7}$ heteromer could provide an important mechanism for the modulation of $P2X_7$ receptor signalling, and so has important consequences for $P2X_7$ as a therapeutic target and for its physiological roles in a range of diseases and immune cell function. We sought to evaluate a molecular basis for its existence using biochemical, functional and pharmacological methods.

Molecular Pharmacology Fast Forward. Published on September 4, 2007 as DOI: 10.1124/mol.107.035980
This article has not been copyedited and formatted. The final version may differ from this version.

Material and Methods

Antibodies and Reagents. The following primary antibodies were used: rabbit polyclonal anti-$P2X_2$ subunit (0.6 µg/ml; Alomone Labs, Jerusalem, Israel), rabbit polyclonal anti-$P2X_4$ subunit (6 µg/ml; Alomone), rabbit polyclonal anti-$P2X_7$ subunit (1.5 µg/ml; Alomone), mouse monoclonal anti-HA (0.8 µg/ml; Roche), rabbit polyclonal anti-EE (1 µg/ml Bethyl, UK), anti-LAMP-1 (0.8 µg/ml, Santa-Cruz Biotechnologies). FITC- or Cy3-conjugated goat anti-mouse or anti-rabbit IgG secondary antibodies (1:250; Jackson Immuno-Research Laboratories, Inc.) were used for immunofluorescence. Horseradish peroxidase-conjugated anti-mouse or anti-rabbit secondary antibodies (1:10000; Amersham Biosciences and Perbio Science, Cramlington, UK) or Rabbit TrueBlot™-Horseradish Peroxidase (HRP) anti-rabbit IgG (eBioscience, US), were used for Western blotting. Complete Protease Inhibitor cocktail (Roche), n-Dodecyl-b-D-maltoside (DDM, Melford Labs, UK), Anti-Rabbit IgG-beads (eBioscience, US) and BCA Protein assay kit (Pierce) were used for co-immunoprecipitation experiments. Sulfo-succinimidyl 2-(biotinamido)-ethyl-1,3'-dithiopropionate was from Pierce, Rockford, IL. Unless otherwise stated, all others reagents were obtained from Sigma or Invitrogen.

DNA Constructs. The construction and characterization of $P2X_4$ and $P2X_2$ receptors with enhanced green fluorescent protein fused to the C-terminus ($P2X_4$-EGFP, $P2X_2$-EGFP) has been previously been described (Bobanovic et al., 2002). Briefly, to generate cDNA encoding $P2X_4$ with EGFP fused to the C terminus, the rat cDNA (a kind gift from Prof. P.P.A Humphrey) was amplified by PCR using oligonucleotide primers to introduce

Molecular Pharmacology Fast Forward. Published on September 4, 2007 as DOI: 10.1124/mol.107.035980
This article has not been copyedited and formatted. The final version may differ from this version.

a Kozak initiation sequence (Kozak, 1987), to remove the stop codon and to introduce *NheI* and *SacII* sites at the 5' and 3' ends, respectively. Amplification products were then cloned into the pEGFP-N1 vector (Clontech, CA). Other constructs used include wild type $P2X_4$ and $P2X_4$ with a hemagglutinin (HA) tag at the C terminus. These sequences were subcloned into the pEGFP-N1 vector so that the enhanced green fluorescent protein (EGFP) sequence was excised. The C353W and S341W point mutations were made using the Quick Change II site directed mutagenesis kit (Stratagene) in $P2X_4$-EGFP. The sequences of all amplified regions were verified using automated DNA sequencing (Department of Genetics, University of Cambridge, UK). Other constructs used include wild-type rat $P2X_7$ and $P2X_2$, $P2X_2$ tagged at its N terminus with HA, pEGFP-N1 and DsRed-ER (Clontech, Mountain View, CA). Glu-Glu (EE)-tagged $P2X_7$ in pcDNA3 was a kind gift from A. Surprenant.

Cell Culture and Transfection. Normal rat kidney (NRK) cells and human embryonic kidney 293 (HEK293) cells were maintained in Dulbecco's modified Eagle's medium (DMEM) containing 10% fetal bovine serum and 100 units/ml penicillin/streptomycin at 37°C and 5% CO_2. Transient transfections of NRK cells were carried out using Lipofectamine 2000 (Invitrogen, Carlsbad, CA), according to the manufacturer's instructions. For transfection of one well of a 12-well plate, 1 µg of plasmid DNA was used. Transient transfections of HEK293 cells were carried out using the modified calcium phosphate method as described previously (Bobanovic et al., 2002). The amount of DNA used to form a precipitate was 3 µg (in 100 µl $CaCl_2$/100 µl 2× HBS) and this was added to cells (200 µl/well) for 6 hours. For co-transfection experiments, equal

Molecular Pharmacology Fast Forward. Published on September 4, 2007 as DOI: 10.1124/mol.107.035980
This article has not been copyedited and formatted. The final version may differ from this version.

amounts of DNA were used and we also included 0.5 µg of pEGFP-N1 vector for co-expression of EGFP with non-fluorescent constructs.

Bone marrow derived macrophages (BMDMs) were obtained from 5-6 week-old, male CD-1 mice. Mice were killed, the femur was excised, and the epiphyses removed prior to flushing out the bone marrow. Cells were washed and resuspended in RPMI 1640 media supplemented with 20% fetal calf serum (FCS), 100U/ml of penicillin/streptomycin and 30% L929 cell-conditioned media. Cells were cultured for 7 days before use and treated for 48 hours with lipopolysaccharide (LPS) solution (1 µg/ml) before membrane protein fraction isolation.

Cell Biology and Immunofluorescence Protocols. Both NRK cells and HEK293 cells were plated onto poly-D-lysine-treated coverslips. All cells were used 24 hours post-transfection. The basic protocol for total staining of the receptors was as follows. Cells were fixed in 3% paraformaldehyde (PFA) and 4% sucrose in PBS (in mM: 1.5 NaH_2PO_4, 8 Na_2HPO_4, and 145 NaCl, pH 7.3) for 10 minutes at 4°C. If required, permeabilisation was done using 0.1% Triton X-100 in PBS for 10 minutes at 4°C. Nonspecific sites were blocked using PBS containing 4% normal goat serum and 3% bovine serum albumin (blocking buffer). Antibodies were diluted to their final concentration in blocking solution. Primary antibodies were applied for 2 hours at room temperature. Cells were rinsed once in blocking buffer and three times for 5 minutes with PBS, and then secondary antibodies were applied for 2 hours at room temperature. Finally, cells were washed five times for 5 minutes with PBS and mounted onto slides with Vectashield (Vector Laboratories, Burlingame, CA) as a mounting medium. In some

Molecular Pharmacology Fast Forward. Published on September 4, 2007 as DOI: 10.1124/mol.107.035980
This article has not been copyedited and formatted. The final version may differ from this version.

experiments 100% methanol was used for 10 minutes at -20°C to fix and permeabilise the cells.

Image Analysis. Fluorescence was visualized using a Zeiss Axiovert LSM510 confocal microscope using a 63× oil immersion objective (Carl Zeiss Inc., Thornwood, NY). For FITC-Cy3 anti-FLAG double labeling, FITC and Cy3 were excited at 7% and 60% of 488 and 543 laser power, respectively. For each experiment, images were collected using identical acquisition parameters and analysed using Image J. Pixel values were on an 8-bit scale (2^8 = 256; 0-255).

Biotinylation. Cells were washed with ice-cold PBS and incubated with 1 mg/ml of sulfo-succinimidyl 2-(biotinamido)-ethyl-1,3'-dithiopropionate for 20 minutes at 4°C. Excess biotin was quenched with PBS containing 50 mM glycine. Cells were solubilised with lysis buffer (20 mM Tris, pH 8.0, 150 mM NaCl, 1 mM EDTA, 2 mM EGTA, 1% NP-40, 1 mM PMSF, 50 mM NaF, 1 mM sodium orthophosphate, 20 mM β-glycerophosphate, 10 mM sodium pyrophosphate, and protease inhibitors) and incubated on ice for 30 minutes, after which time they were sonicated and cleared by centrifugation. The majority of the supernatant was incubated with immobilised NeutrAvidin biotin binding protein beads (Pierce) on a rotating rack for 2 hours at 4°C to precipitate biotinylated proteins. The remaining supernatant was kept to assess total protein in each sample. Beads containing precipitated biotinylated proteins were spun for 1 minute at 10,000 rpm at 4°C and washed at least three times. The protein was eluted from the beads by incubation in 20 µl of the Laemmli buffer. Proteins were separated by SDS-PAGE by loading on 7.5% polyacrylamide gels and detected by immunoblotting. The $P2X_4$

Molecular Pharmacology Fast Forward. Published on September 4, 2007 as DOI: 10.1124/mol.107.035980
This article has not been copyedited and formatted. The final version may differ from this version.

receptor was detected using a rabbit polyclonal anti-$P2X_4$ antibody (1:500). The $P2X_7$ receptor was detected using a rabbit polyclonal anti-$P2X_7$ antibody (1:100). Immunoreactive bands were visualized using appropriate horseradish peroxidase-conjugated secondary antibodies followed by enhanced chemiluminescence detection. All blots shown in figures are typical of at least two and in most cases four similar results.

Membrane protein fraction isolation. In order to obtain total membrane protein fractions for immunoprecipitation assays, transfected HEK293 cells or bone marrow derived macrophages (BMDMs) were washed three times with HBS-EDTA buffer (50 mM HEPES pH 7.4, 100 mM NaCl, 2 mM EDTA), scrapped off, and then collected by gentle centrifugation. The cell pellet was resuspended in ice-cold hypotonic buffer (10 mM Tris-HCl pH 7.0, 2 mM EDTA, 1 mM PMSF and Protease Inhibitors cocktail) and incubated for 20 minutes on ice. Cells were mechanically disrupted by passing the solution through a needle, and then the extract was centrifuged at high speed (14000 rpm, 15 minutes). The pellet containing the membrane-derived protein fraction was solubilised using 1% DDM in HBS buffer for 1 hour on ice and the solution was ultracentrifuged at 30000 rpm for 1hour. The membrane protein fraction was collected from the supernatant and subjected to the BCA protein assay.

Immunoprecipitation. Total membrane protein extracts were pre-absorbed with Anti-Rabbit IgG-beads for 30 minutes. The pre-cleared membrane protein extracts were then incubated with 2-5 μg of anti-$P2X_4$ or anti-$P2X_7$ antibody in HBS buffer containing 1% DDM for 2 hours at 4°C. Anti-Rabbit IgG beads were subsequently added to the samples and the mixture was further incubated for 1hour at 4°C. The protein-beads complexes were washed four times with HBS buffer containing 1% DDM and proteins were eluted

Molecular Pharmacology Fast Forward. Published on September 4, 2007 as DOI: 10.1124/mol.107.035980
This article has not been copyedited and formatted. The final version may differ from this version.

by boiling for 5 minutes in 40 μl of Laemmli buffer. Samples were analyzed by SDS-PAGE and probed by Western blot using the corresponding primary antibody and Rabbit TrueBlot™-Horseradish Peroxidase (HRP) anti-rabbit IgG as secondary antibody. When the immunoprecipitation was performed using a monoclonal anti-HA antibody, protein G-beads were used instead to isolate the complexes, and a HRP-anti-mouse secondary antibody was employed for detection in Western blots.

Electrophysiological Recordings. Standard whole-cell recordings were performed at room temperature using an Axopatch 200A amplifier (Axon Instruments, Inc.). Patch pipettes (3-6 megaohms) were pulled from thick-walled borosilicate glass (GC150F-10, Harvard Apparatus, Inc.). ATP-induced responses were measured at -30 mV, and different extracellular (EC) solutions were used. These included normal Na^+ EC solution (in mM: 140 NaCl, 5 KCl, 2 $CaCl_2$, 1 $MgCl_2$, 10 D-glucose and 10 HEPES, pH 7.3); Na^+ EC solution with low divalent (in mM: 151 NaCl, 0.3 $CaCl_2$, 10 HEPES and 10 Glucose, pH 7.3); Cs^+ EC solution with low divalent (in mM: 151 CsCl, 0.3 $CaCl_2$, 10 HEPES and 10 Glucose, pH 7.3); Cs^+ EC solution with 1.58 mM Ca^{2+} (in mM: 151 CsCl, 1.58 $CaCl_2$, 10 HEPES and 10 Glucose, pH 7.3); Cs^+ + Na^+ EC solution with low divalent (in mM: 121 CsCl, 30 NaCl, 0.3 $CaCl_2$, 10 HEPES and 10 Glucose, pH 7.3). When using Na^+ EC solution the intracellular (IC) solution had the following composition (in mM: 70 K_2SO4, 10 KCl, 1 $MgCl_2$, 10 HEPES and 75 sucrose, pH 7.3). When using a Cs^+ EC solution the composition of the IC solution was as follows (in mM: 151 CsCl, 10 HEPES, 0.1 EGTA, pH 7.3).

Molecular Pharmacology Fast Forward. Published on September 4, 2007 as DOI: 10.1124/mol.107.035980
This article has not been copyedited and formatted. The final version may differ from this version.

Whole-cell currents were low pass-filtered at 2 kHz and digitized at 10 kHz. Agonists were applied locally using a Picospritzer II (Parker Instrumentation). To ensure delivery of drug, 0.05% (w/v) fast green was used. (Local applications of 1% fast green induced no response.) To visualize cells expressing P2X receptors without an EGFP tag, cells were cotransfected with EGFP. Cells expressing EGFP or EGFP-tagged P2X subunits were observed under a microscope with an epifluorescence attachment (Nikon, Tokyo, Japan). Untransfected cells and cells expressing EGFP alone were found to have no inward current in response to application of agonists. Acquisition was performed using HEKA Pulse Version 8.30, and data were subsequently analyzed using IgorPRO Version 3.16. Statistical analyses were performed with Student's unpaired *t* test.

Molecular Pharmacology Fast Forward. Published on September 4, 2007 as DOI: 10.1124/mol.107.035980
This article has not been copyedited and formatted. The final version may differ from this version.

Results

Co-expression of $P2X_4$ and $P2X_7$ increased the surface expression of $P2X_4$.

We examined the distribution of $P2X_4$ and $P2X_7$ when expressed either individually or together in HEK293 and NRK cells using immunocytochemical labelling. We previously showed that $P2X_4$ receptors undergo rapid and constitutive endocytosis and reside predominantly within intracellular compartments (Bobanovic et al., 2002; Royle et al., 2002). Figure 1 shows $P2X_4$ co-localized with the lysosomal marker, Lamp-1, whereas $P2X_7$ receptors containing a Glu-Glu tag at the C-terminus ($P2X_7$-EE) were predominantly co-localized with the ER maker, DsRed-ER (Fig. 1A). Using methanol rather than PFA to fix the cells enhanced antibody labelling of $P2X_7$ at the plasma membrane (Fig. 1B). When $P2X_4$ and $P2X_7$ were co-expressed in NRK cells, $P2X_4$ was still predominantly within endolysosomes and there was very little labelling of $P2X_7$-EE in these compartments, suggesting that these receptors are $P2X_4$ homomers. At the plasma membrane, however, there was overlap in the distribution of the two receptors. To look at any change in the surface expression of $P2X_4$ and $P2X_7$, surface proteins were biotinylated and analysed by western blot (Fig. 1, C and D). The biotinylated fraction of $P2X_4$ increased ~2-fold in the presence of $P2X_7$, although total $P2X_4$ levels did not change, suggesting that association with $P2X_7$ stabilises $P2X_4$ at the plasma membrane. In contrast, there was no change in the surface expression of $P2X_7$ with and without $P2X_4$.

Molecular Pharmacology Fast Forward. Published on September 4, 2007 as DOI: 10.1124/mol.107.035980
This article has not been copyedited and formatted. The final version may differ from this version.

Association of $P2X_4$ and $P2X_7$ receptor subunits.

To test whether or not $P2X_7$ receptor subunits can associate with $P2X_4$ receptor subunits, we performed immunoprecipitation (IP) experiments using HEK293 cells cotransfected with $P2X_7$ and $P2X_4$. Membrane proteins were solubilized using 1% n-Dodecyl-D-maltoside (DDM) as this was more effective at solubilizing $P2X_7$ than 1% Triton X-100, NP-40 or CHAPs (data not shown). Following IP of the receptor complex using anti-$P2X_4$ antibody, $P2X_7$ was detected by immunoblotting with anti-$P2X_7$ antibody (Fig. 2A) but only when $P2X_4$ was also present. We also co-expressed $P2X_4$-HA with $P2X_7$ and were able to co-IP $P2X_7$ with anti-HA antibody (Fig. 2B). This gel shows that although two bands were detected for $P2X_7$ in the membrane fraction, which presumably represent fully and partially glycosylated forms, only the higher band was detected after co-IP. This suggests that the complex formed by $P2X_4$ and $P2X_7$ is not a misagregate that is retained in the ER, but instead is trafficked along the secretory pathway to the trans golgi network and presumably from there to the plasma membrane.

Having shown that overexpressed $P2X_4$ and $P2X_7$ associate with one another we next tested whether or not the endogenous receptors in bone marrow derived macrophages could be co-immunoprecipitated. We performed the co-IP with anti-$P2X_4$ and the immunoblot with anti-$P2X_7$ and were able to detect a clear band running at the appropriate size for $P2X_7$ (Fig. 2C). Thus native $P2X_4$ and $P2X_7$ receptors in mouse macrophages associate to form part of the same complex.

Molecular Pharmacology Fast Forward. Published on September 4, 2007 as DOI: 10.1124/mol.107.035980
This article has not been copyedited and formatted. The final version may differ from this version.

A functional interaction between $P2X_4$ and $P2X_7$ receptors

To investigate the functional significance of the interaction between $P2X_4$ and $P2X_7$ subunits we utilized two non-functional $P2X_4$ receptor mutants, C353W and S341W, which were previously characterized in *Xenopus* oocytes (Silberberg et al., 2005). When expressed alone in oocytes neither mutant produced a current in response up to 300 μM ATP although their surface expression was equivalent to the wild type (wt) $P2X_4$ receptor, indicating that the mutations interfered with channel functional and not maturation or trafficking. When co-expressed with wt $P2X_4$, the C353W mutant dramatically reduced the currents whereas the S341W mutant had no inhibitory effect (Silberberg et al., 2005). We obtained very similar results using the EGFP-tagged mutants, expressed alone or with wt $P2X_4$ in HEK293 cells (Fig. 3A). Both mutants expressed individually were non-functional in response to 30-100 μM ATP and when coexpressed with wt $P2X_4$, the C353W mutant reduced the peak current amplitude by ~75%, whereas the S341W mutant produced a small, but not significant potentiation. We next compared the effect of these mutants on the current carried by the wt $P2X_7$ receptor (Fig. 3B). The $P2X_4$C353W mutant inhibited the $P2X_7$ receptor currents evoked by 1 mM ATP^{4-} by greater than 50% but the currents recorded from cells co-expressing the S341W mutant with $P2X_7$ were slightly increased compared to $P2X_7$ alone. Similar results were obtained with 100 μM ATP^{4-} and also with the $P2X_7$ receptor preferred agonist, BzATP (Fig 3C). We compared the BzATP dose response relationship for $P2X_7$ alone and $P2X_7$ coexpressed with the S341W mutant and the EC_{50} values were similar (11.4±1.1 μM and 9.1±0.8 μM respectively) (Fig 3D). In contrast the wt $P2X_4$ receptor produced very little response to BzATP up to concentrations of 100 μM. Neither the S341W nor C353W

Molecular Pharmacology Fast Forward. Published on September 4, 2007 as DOI: 10.1124/mol.107.035980
This article has not been copyedited and formatted. The final version may differ from this version.

mutants altered the surface expression of $P2X_7$ as measured by biotinylating surface proteins (Fig. 3E), indicating that functional inhibition of $P2X_7$ by the C353W mutant was not caused by a reduction in the number of receptors reaching the plasma membrane. If we assume that association of the C353W mutant with $P2X_7$ abolishes receptor function, as suggested for receptors formed from wt $P2X_4$ and the C353W mutant, then we can estimate that there was a >2-fold reduction in the number of functional homomeric $P2X_7$ receptors at the plasma membrane in the presence of the C353W mutant. This suggests that more than half of the surface $P2X_7$ receptor subunits were associated with the $P2X_4$C353W mutant. In contrast to the inhibition of $P2X_7$ by $P2X_4$C353W, there was no change in $P2X_2$ receptor currents upon co-expression with either $P2X_4$C353W or S341W (Fig 3F).

Having demonstrated an interaction between the $P2X_4$ mutants and wt $P2X_7$ we tested how co-expression of wt $P2X_4$ and $P2X_7$ affected the responses to BzATP and MgATP (Fig. 4, A and B). MgATP activated large currents in cells expressing $P2X_4$ alone and BzATP activated large currents in cells expressing the $P2X_7$ receptor. In cells co-expressing these receptors, summation of the response produced by each receptor expressed individually would suggest two independent pools of homomeric receptors. The currents evoked by both agonists were, however, significantly reduced compared to what one would predict for a simple summation suggesting a functional interaction between the two receptors. This was not the case for $P2X_2$ and $P2X_7$ (Fig. 4C), and the apparent lack of a functional interaction between these two subtypes was consistent with their inability to co-IP (Supplementary Fig. 1).

Molecular Pharmacology Fast Forward. Published on September 4, 2007 as DOI: 10.1124/mol.107.035980
This article has not been copyedited and formatted. The final version may differ from this version.

Co-expression of $P2X_4$ with $P2X_7$ confers ivermectin (IVM) sensitivity to BzATP evoked currents

To further test whether or not an interaction between $P2X_4$ and $P2X_7$ alters the functional properties of the receptors we compared some of their pharmacological properties when expressed individually and together. $P2X_7$ receptors have been shown to be sensitive to extracellular (EC) Na^+ (Ma et al., 2006). Substituting Cs^+ for Na^+ in the EC solution slowed the activation and deactivation kinetics of $P2X_7$ receptor currents and enhanced the difference in its time course compared with $P2X_4$ receptor currents (Fig. 5). It also potentiated the amplitude of both BzATP-evoked $P2X_7$ receptor currents and currents recorded from cells co-expressing $P2X_4$ and $P2X_7$ (Supplementary Fig. 2), whereas there was minimal activation of $P2X_4$ receptors using 3 μM BzATP (Fig 5A). Ivermectin (IVM) is an allosteric modulator of $P2X_4$ receptors that augments currents by stabilizing the agonist-induced open state (Priel & Silberberg 2004). We tested its effects on BzATP evoked currents and whereas there was no effect on currents from cells transfected with $P2X_7$ alone, in cells co-expressing $P2X_4$ and $P2X_7$ the currents were potentiated >2-fold following prior incubation with IVM. This suggests that association of $P2X_4$ with $P2X_7$ confers IVM sensitivity to the receptor although this interpretation is confounded by the finding that BzATP is a much more effective agonist at homomeric $P2X_4$ receptors following IVM treatment. The time course of the $P2X_4$ receptor currents differed however from those recorded from cell co-expressing the two receptors. In order to remove any component of the whole cell current that was mediated by $P2X_4$ homomeric receptors a similar experiment was performed but using the $P2X_4$S341W mutant coexpressed with $P2X_7$. This mutant expressed alone was non-functional with and

Molecular Pharmacology Fast Forward. Published on September 4, 2007 as DOI: 10.1124/mol.107.035980
This article has not been copyedited and formatted. The final version may differ from this version.

without IVM pre-treatment but conferred IVM sensitivity to BzATP-evoked currents recorded from cells co-expressing this mutant with $P2X_7$ (Fig. 5B). Similar results were obtained with Na^+ EC solution (Fig. 5C) and using MgATP as the agonist, although the currents were much smaller (Fig. 5D).

TNP-ATP and Brilliant Blue G (BBG) inhibit $P2X_{4/7}$ receptor currents

We next tested the effects of the $P2X_4$ receptor antagonist, TNP-ATP, and the $P2X_7$ receptor antagonist BBG (Tsuda et al., 2003; Virginio et al., 1998; Jiang et al., 2000). TNP-ATP (2 μM) inhibited MgATP-activated $P2X_4$ receptor currents by ~70% but had no significant effect on the amplitude of BzATP-evoked $P2X_7$ receptor currents. In contrast it significantly inhibited BzATP-evoked currents from cell co-expressing $P2X_4$ and $P2X_7$ (Fig. 6A). At this concentration of BzATP, $P2X_4$ homomeric receptor currents are not expected to make a significant contribution to the whole cell current amplitude, however to rule out the possibility that there was a significant $P2X_4$ receptor mediated component, the experiment was repeated using the S341W mutant. Currents recorded from cells co-expressing $P2X_4$ S341W and $P2X_7$ were reduced by ~70% following incubation with TNP-ATP.

Finally we tested the effects of BBG which almost completely abolished BzATP-activated $P2X_7$ receptor currents, but had very little effect at $P2X_4$ receptors (Fig. 6B). It substantially reduced currents recorded from cells co-expressing $P2X_7$ and $P2X_4$ S341W, although these were significantly less sensitive as judged by the amplitude of the BzATP evoked response following a 10 minutes incubation with 1 μM BBG.

Molecular Pharmacology Fast Forward. Published on September 4, 2007 as DOI: 10.1124/mol.107.035980
This article has not been copyedited and formatted. The final version may differ from this version.

Discussion

The $P2X_7$ receptor represents an important therapeutic target in a number of diseases such as stroke and arthritis pain. ATP-mediated responses in native tissues are frequently ascribed to $P2X_7$ however often display characteristics that are shared by other P2X receptors (Inoue, 2006; North, 2002). A molecular basis for these responses has not been established because the $P2X_7$ receptor is not thought to associate with any other P2X subunits. Our results provide evidence that the $P2X_7$ receptor can associate with another P2X subunit, which has an emerging role in pain and inflammation, namely $P2X_4$ (Guo and Schluesener, 2005; Inoue et al., 2004; Tsuda et al., 2003). This interaction was demonstrated not only in HEK293 cells overexpressing both receptors, but also endogenously, for native receptors present in primary cultures of BMDMs. Our results differ from those of an earlier study which failed to co-IP $P2X_4$ and $P2X_7$ from HEK293 cells (Torres et al., 1999). A possible explanation is the use of different detergents; we used DDM, which often preserves protein activity better than other detergents including NP-40. The association with $P2X_7$ affected the trafficking properties of $P2X_4$, increasing its stability at the plasma membrane, although it was still predominantly located within intracellular compartments. Co-expression with a dominant negative mutant of $P2X_4$, (C353W), knocked down $P2X_7$ receptor currents by >50% without reducing its surface expression, suggesting that more than half of the surface $P2X_7$ subunits were in complexes associated with the C353W mutant. By using a non-functional but non-dominant negative $P2X_4$ mutant we provide evidence that a heteromer formed from $P2X_4$ and $P2X_7$ has properties in common with both of the parent homomeric receptors. A question that remains to be answered is whether or not $P2X_4$ and $P2X_7$ subunits

Molecular Pharmacology Fast Forward. Published on September 4, 2007 as DOI: 10.1124/mol.107.035980
This article has not been copyedited and formatted. The final version may differ from this version.

coassemble to form heterotrimeric structures with a common central conduction pore. In light of our findings, however, the prevailing hypothesis of $P2X_7$ receptors as unique members within the P2X family forming exclusively stable homotrimers seems unlikely to be correct.

The identification of novel functional properties that cannot be attributed to the parent homomeric receptors is a well established approach for demonstrating heteromerization between different members of the same family of receptor. In this study, in order to distinguish between homomeric and heteromeric receptor currents we took advantage of a $P2X_4$ receptor mutant (S341W) which, although non functional when expressed alone, had previously been shown to traffic to the surface in the normal way and to produce no inhibition of wt $P2X_4$ receptor currents (Silberberg et al., 2005). When coexpressed with wt $P2X_7$, this mutant produced a small potentiation of BzATP and ATP^{4-} evoked currents and we have made the assumption that currents with $P2X_4$-like pharmacological properties were mediated by a heteromer composed of $P2X_4$S341W and $P2X_7$. Our conclusions are that the heteromeric receptors are preferentially activated by BzATP compared with MgATP, they are allosterically modulated by IVM and inhibited by both TNP-ATP and BBG. In Cs^+ EC solution, the IVM-sensitive component of the whole cell current was larger in amplitude and with slower activation and deactivation kinetics than in Na^+ EC solution suggesting that the $P2X_{4/7}$ complex is inhibited by EC Na^+ similar to $P2X_7$ homomeric receptors. The increase in receptor diversity as a result of functional heteromeric as well as homomeric P2X receptors being expressed in cells such as macrophages and microglia, which predominantly express $P2X_4$ and $P2X_7$, clearly has

Molecular Pharmacology Fast Forward. Published on September 4, 2007 as DOI: 10.1124/mol.107.035980
This article has not been copyedited and formatted. The final version may differ from this version.

implications for the development of new therapies that target purinergic receptors for the treatment of neuropathic pain.

$P2X_4$ and $P2X_7$ are co-expressed in epithelial and endothelial cells as well as immune cells (Bowler et al., 2003; Ma et al., 2006; Xiang and Burnstock, 2005). In airway epithelia, P2X receptor agonists stimulate Cl^- transport across nasal mucosa and are involved in the regulation of ciliary beat (Hayashi et al., 2005; Zsembery et al., 2004). Manipulation of both of these processes may be of therapeutic benefit for patients with cystic fibrosis and defining the subunit identity and functional properties of the native receptors is important if these receptors are to be targeted for CF therapy. Ma et al. (2006) described the pharmacological features of the P2X receptor in airway ciliated cells and several properties are similar to what we report here for the heterologously co-expressed receptors. The native receptor currents were inhibited by BBG and EC Na^+, and augmented by IVM. Based upon this pharmacological profile they hypothesized that the P2X receptor in ciliated cells is an assembly of $P2X_4$ and $P2X_7$ subunits, which is supported by our results.

The association between $P2X_4$ and $P2X_7$ may alter downstream signalling pathways, for example activation of the MAP kinase cascade (Donnelly-Roberts et al., 2004), phosphatidylserine translocation (Dutot et al., 2006) and coupling to ABC transporters (Marty et al., 2005). The hemichannel pannexin-1 was recently shown to form a complex with $P2X_7$ and to play an important role in coupling activation of the receptor to increased membrane permeability to large molecules such as ethidium, and to IL-1β

synthesis and release (Pelegrin and Surprenant, 2006). Whether or not pannexin-1 can functionally couple with $P2X_{4/7}$ receptors remains to be established. Our results provide a molecular basis for the existence of $P2X_{4/7}$ receptors and further studies will be required to elucidate the precise nature of the interaction between the constitutive subunits. These data also present functional significance for the heteromeric assembly between $P2X_4$ and $P2X_7$ and we foresee the importance of this interaction in purinergic receptor-mediated signalling of pain in health and disease.

Molecular Pharmacology Fast Forward. Published on September 4, 2007 as DOI: 10.1124/mol.107.035980
This article has not been copyedited and formatted. The final version may differ from this version.

Acknowledgements

The assistance of A. Paramasivan in the preparation of BMDMs cells is gratefully acknowledged.

Molecular Pharmacology Fast Forward. Published on September 4, 2007 as DOI: 10.1124/mol.107.035980
This article has not been copyedited and formatted. The final version may differ from this version.

References

Barrera NP, Ormond SJ, Henderson RM, Murrell-Lagnado RD and Edwardson JM (2005) Atomic force microscopy imaging demonstrates that P2X2 receptors are trimers but that P2X6 receptor subunits do not oligomerize. *J Biol Chem* **280**(11):10759-10765.

Bobanovic LK, Royle SJ and Murrell-Lagnado RD (2002) P2X receptor trafficking in neurons is subunit specific. *J Neurosci* **22**(12):4814-4824.

Bowler JW, Bailey RJ, North RA and Surprenant A (2003) P2X4, P2Y1 and P2Y2 receptors on rat alveolar macrophages. *Br J Pharmacol* **140**(3):567-575.

Chessell IP, Hatcher JP, Bountra C, Michel AD, Hughes JP, Green P, Egerton J, Murfin M, Richardson J, Peck WL, Grahames CB, Casula MA, Yiangou Y, Birch R, Anand P and Buell GN (2005) Disruption of the P2X7 purinoceptor gene abolishes chronic inflammatory and neuropathic pain. *Pain* **114**(3):386-396.

Dell'Antonio G, Quattrini A, Dal Cin E, Fulgenzi A and Ferrero ME (2002) Antinociceptive effect of a new P(2Z)/P2X7 antagonist, oxidized ATP, in arthritic rats. *Neurosci Lett* **327**(2):87-90.

Donnelly-Roberts DL, Namovic MT, Faltynek CR and Jarvis MF (2004) Mitogen-activated protein kinase and caspase signaling pathways are required for P2X7 receptor (P2X7R)-induced pore formation in human THP-1 cells. *J Pharmacol Exp Ther* **308**(3):1053-1061.

Dutot M, Pouzaud F, Larosche I, Brignole-Baudouin F, Warnet JM and Rat P (2006) Fluoroquinolone eye drop-induced cytotoxicity: role of preservative in P2X7 cell death receptor activation and apoptosis. *Invest Ophthalmol Vis Sci* **47**(7):2812-2819.

Gu BJ and Wiley JS (2006) Rapid ATP-induced release of matrix metalloproteinase 9 is mediated by the P2X7 receptor. *Blood* **107**(12):4946-4953.

Guo LH and Schluesener HJ (2005) Lesional accumulation of P2X(4) receptor(+) macrophages in rat CNS during experimental autoimmune encephalomyelitis. *Neuroscience* **134**(1):199-205.

Hayashi T, Kawakami M, Sasaki S, Katsumata T, Mori H, Yoshida H and Nakahari T (2005) ATP regulation of ciliary beat frequency in rat tracheal and distal airway epithelium. *Exp Physiol* **90**(4):535-544.

Humphreys BD, Rice J, Kertesy SB and Dubyak GR (2000) Stress-activated protein kinase/JNK activation and apoptotic induction by the macrophage P2X7 nucleotide receptor. *J Biol Chem* **275**(35):26792-26798.

Inoue K (2006) The function of microglia through purinergic receptors: Neuropathic pain and cytokine release. *Pharmacol Ther* **109**(1-2):210-226.

Inoue K, Tsuda M and Koizumi S (2004) ATP- and adenosine-mediated signaling in the central nervous system: chronic pain and microglia: involvement of the ATP receptor P2X4. *J Pharmacol Sci* **94**(2):112-114.

Jiang LH, Mackenzie AB, North RA and Surprenant A (2000) Brilliant blue G selectively blocks ATP-gated rat P2X(7) receptors. *Mol Pharmacol* **58**(1):82-88.

Jiang LH, Rassendren F, Mackenzie A, Zhang YH, Surprenant A and North RA (2005) N-methyl-D-glucamine and propidium dyes utilize different permeation pathways at rat P2X(7) receptors. *Am J Physiol Cell Physiol* **289**(5):C1295-1302.

Khakh BS and North RA (2006) P2X receptors as cell-surface ATP sensors in health and disease. *Nature* **442**(7102):527-532.

King BF, Townsend-Nicholson A, Wildman SS, Thomas T, Spyer KM and Burnstock G (2000) Coexpression of rat P2X2 and P2X6 subunits in Xenopus oocytes. *J Neurosci* **20**(13):4871-4877.

Kozak M (1987) At least six nucleotides preceding the AUG initiator codon enhance translation in mammalian cells. *J Mol Biol* **196**(4):947-950.

Labasi JM, Petrushova N, Donovan C, McCurdy S, Lira P, Payette MM, Brissette W, Wicks JR, Audoly L and Gabel CA (2002) Absence of the P2X7 receptor alters leukocyte function and attenuates an inflammatory response. *J Immunol* **168**(12):6436-6445.

Lewis C, Neidhart S, Holy C, North RA, Buell G and Surprenant A (1995) Coexpression of P2X2 and P2X3 receptor subunits can account for ATP-gated currents in sensory neurons. *Nature* **377**(6548):432-435.

Ma W, Korngreen A, Weil S, Cohen EB, Priel A, Kuzin L and Silberberg SD (2006) Pore properties and pharmacological features of the P2X receptor channel in airway ciliated cells. *J Physiol* **571**(Pt 3):503-517.

Marty V, Medina C, Combe C, Parnet P and Amedee T (2005) ATP binding cassette transporter ABC1 is required for the release of interleukin-1beta by P2X7-stimulated and lipopolysaccharide-primed mouse Schwann cells. *Glia* **49**(4):511-519.

Nicke A, Kerschensteiner D and Soto F (2005) Biochemical and functional evidence for heteromeric assembly of P2X1 and P2X4 subunits. *J Neurochem* **92**(4):925-933.

North RA (2002) Molecular physiology of P2X receptors. *Physiol Rev* **82**(4):1013-1067.

Ormond SJ, Barrera NP, Qureshi OS, Henderson RM, Edwardson JM and Murrell-Lagnado RD (2006) An uncharged region within the N terminus of the P2X6 receptor inhibits its assembly and exit from the endoplasmic reticulum. *Mol Pharmacol* **69**(5):1692-1700.

Pelegrin P and Surprenant A (2006) Pannexin-1 mediates large pore formation and interleukin-1beta release by the ATP-gated P2X7 receptor. *Embo J* **25**(21):5071-5082.

Perregaux DG, McNiff P, Laliberte R, Conklyn M and Gabel CA (2000) ATP acts as an agonist to promote stimulus-induced secretion of IL-1 beta and IL-18 in human blood. *J Immunol* **165**(8):4615-4623.

Priel A and Silbergberg SD (2004) Mechanism of ivermectin facilitation of human P2X4 receptor channels. *J Gen Physiol* 123 (3): 281-293.

Royle SJ, Bobanovic LK and Murrell-Lagnado RD (2002) Identification of a non-canonical tyrosine-based endocytic motif in an ionotropic receptor. *J Biol Chem* **277**(38):35378-35385.

Silberberg SD, Chang TH and Swartz KJ (2005) Secondary structure and gating rearrangements of transmembrane segments in rat P2X4 receptor channels. *J Gen Physiol* **125**(4):347-359.

Torres GE, Egan TM and Voigt MM (1999) Hetero-oligomeric assembly of P2X receptor subunits. Specificities exist with regard to possible partners. *J Biol Chem* **274**(10):6653-6659.

Tsuda M, Shigemoto-Mogami Y, Koizumi S, Mizokoshi A, Kohsaka S, Salter MW and Inoue K (2003) P2X4 receptors induced in spinal microglia gate tactile allodynia after nerve injury. *Nature* **424**(6950):778-783.

Virginio C, Robertson G, Surprenant A and North RA (1998) Trinitrophenyl-substituted nucleotides are potent antagonists selective for P2X1, P2X3, and heteromeric P2X2/3 receptors. *Mol Pharmacol* **53**(6):969-973.

Wilson HL, Wilson SA, Surprenant A and North RA (2002) Epithelial membrane proteins induce membrane blebbing and interact with the P2X7 receptor C terminus. *J Biol Chem* **277**(37):34017-34023.

Xiang Z and Burnstock G (2005) Expression of P2X receptors on rat microglial cells during early development. *Glia* **52**(2):119-126.

Zsembery A, Fortenberry JA, Liang L, Bebok Z, Tucker TA, Boyce AT, Braunstein GM, Welty E, Bell PD, Sorscher EJ, Clancy JP and Schwiebert EM (2004) Extracellular zinc and ATP restore chloride secretion across cystic fibrosis airway epithelia by triggering calcium entry. *J Biol Chem* **279**(11):10720-10729.

Molecular Pharmacology Fast Forward. Published on September 4, 2007 as DOI: 10.1124/mol.107.035980
This article has not been copyedited and formatted. The final version may differ from this version.

Footnotes

This work was supported by the Biotechnology and Biological Sciences Research Council.

Reprint requests to:

Dr Ruth Murrell-Lagnado

Department of Pharmacology

Tennis Court Road

Cambridge

CB2 1PD

UK

Email: rdm1003@cam.ac.uk

Molecular Pharmacology Fast Forward. Published on September 4, 2007 as DOI: 10.1124/mol.107.035980
This article has not been copyedited and formatted. The final version may differ from this version.

Legends for Figures

Fig. 1.

Co-expression of $P2X_7$ and $P2X_4$ increased $P2X_4$ at the plasma membrane. A, confocal images of HEK293 cells transfected with either $P2X_4$ or $P2X_7$. $P2X_4$ receptors (green) were co-localized with LAMP-1 (red) and $P2X_7$ receptors (green) were co-localized with an ER marker, DsRed-ER. Cells were fixed with 3% PFA and permeabilised with 0.1% Triton X-100 in PBS for 10 minutes at 4°C. **B**, NRK cells transfected with either $P2X_7$ or $P2X_4$ alone (top panel) or co-transfected with $P2X_7$ and $P2X_4$-EGFP (lower panel) were fixed with 100% methanol. Methanol fixation increased the detection of $P2X_7$ at the plasma membrane. In co-transfected cells there was overlap between $P2X_4$ and $P2X_7$ at the plasma membrane. Scale bars, 10 μm. **C**, transfected NRK cells were incubated with biotin (1 mg/ml) for 20 minutes at 4°C to label surface proteins and were then solubilized and surface proteins precipitated with streptavidin beads. Surface expression of $P2X_4$ increased in the presence of $P2X_7$ (n = 4) although totals show equivalent $P2X_4$ expression. **D**, surface expression of $P2X_7$ was unchanged in the presence of $P2X_4$; in both cases the proportion biotinylated was ~10% of the total $P2X_7$. The first lane shows no detectable expression of $P2X_7$ in untransfected cells.

Molecular Pharmacology Fast Forward. Published on September 4, 2007 as DOI: 10.1124/mol.107.035980
This article has not been copyedited and formatted. The final version may differ from this version.

Fig. 2.

$P2X_7$ and $P2X_4$ subunits physically associate both when overexpressed in HEK293 cells and in native tissue, as shown by co-immunoprecipitation. A, HEK293 cells were transfected with $P2X_4$ and $P2X_7$, or $P2X_7$ alone, and membrane protein complexes were immunoprecipitated with the anti-$P2X_4$ antibody, separated by SDS-PAGE and immunoblotted with anti-$P2X_4$ (left) and anti-$P2X_7$ (right) polyclonal antibodies. The total membrane protein fractions (input, 2.5 μg) were also blotted with the same antibodies for comparison. **B**, cells were co-transfected with $P2X_4$-HA and $P2X_7$, or $P2X_7$ alone, and membrane proteins were immunoprecipitated with an anti-HA antibody, showing that the complex can be isolated via a non P2X-specific antibody. Blots were performed with anti-$P2X_7$ (left) and anti-HA (right) antibodies. **C,** membrane protein fractions isolated from mice bone marrow derived macrophages (BMDMs) were subjected to immunoprecipitation with the anti-$P2X_4$ antibody and the isolated complex was resolved by SDS-PAGE and blotted with both anti-$P2X_4$ (left) and anti-$P2X_7$ (right) antibodies, demonstrating the physical association between $P2X_4$ and $P2X_7$ in native tissue.

Fig. 3.

Inhibition of $P2X_7$ receptor function by co-expression with a dominant negative $P2X_4$ mutant. A, whole-cell patch-clamp recordings were carried out on HEK293 cells expressing $P2X_4$ alone or together with either the $P2X_4$C353W or $P2X_4$S341W mutants. The mutants were also expressed alone. Mutants were tagged with EGFP to enable the transfected cells to be detected. Inward currents, evoked by 30 μM MgATP at a holding

Molecular Pharmacology Fast Forward. Published on September 4, 2007 as DOI: 10.1124/mol.107.035980
This article has not been copyedited and formatted. The final version may differ from this version.

potential of -30 mV were measured in normal Na^+ EC solution. The histogram shows the normalized, mean peak current densities (mean ± S.E.M., $n > 8$). **B**, similar experiments were carried out, co-expressing $P2X_7$ and the $P2X_4$C353W and S341W mutants. Currents were evoked by applying 1 mM ATP^{4-} in Na^+ EC solution with a low divalent cation concentration, at a holding potential of -30 mV. Histogram on the right shows a comparison of the normalized peak current densities (mean ± S.E.M., $n > 10$). **C**, similar results were obtained using either ATP^{4-} (100-1000 μM) or BzATP (10-100 μM). **D**, concentration-response curves for BzATP in HEK293 cells expressing $P2X_7$, $P2X_7$ and $P2X_4$ S341W or P2X4 alone. The data were fit with a Hill equation and the EC_{50} values obtained were 11 ± 1 μM BzATP for $P2X_7$ and 9.1 ± 0.8 μM BzATP for $P2X_7$ with $P2X_4$ S341W (n=4-7), and the correspondent Hill slopes were 1.7 ± 0.2 and 2.0 ± 0.3, respectively. **E**, the surface expression of $P2X_7$, as measured by biotinylation of surface proteins at 4°C, was unchanged in the presence of the two $P2X_4$ mutants. **F**, co-expression of the $P2X_4$ mutants with $P2X_2$ did not inhibit $P2X_2$-receptor mediated currents evoked by 30 μM ATP (mean ± S.E.M., $n > 10$). *$p < 0.05$, **$p < 0.01$, and ***$p < 0.001$.

Fig. 4.

$P2X_4$ but not $P2X_2$ functionally interacts with $P2X_7$. Whole cell currents were recorded from HEK293 cells expressing the constructs shown. Normalized mean current densities are for $n > 8$ for each condition and V_h=-30 mV. **A**, inward currents were evoked by 10 μM BzATP in Na^+ EC solution with low divalent. **B-C**, inward currents were evoked by 200 μM MgATP in Na^+ EC solution with 1.58 mM Ca^{2+}.

Molecular Pharmacology Fast Forward. Published on September 4, 2007 as DOI: 10.1124/mol.107.035980
This article has not been copyedited and formatted. The final version may differ from this version.

Fig. 5.

$P2X_{4/7}$ receptor currents were potentiated by IVM. Whole-cell patch-clamp recordings from HEK293 cells expressing the constructs indicated with and without pre-incubation with 3 μM IVM for 5 minutes. V_h=-30 mV. All histograms represent peak current densities (mean ± S.E.M., *n* > 10). **A**, **B**, Recordings were made in Cs^+ EC solution with low divalent cations in response to 3 μM BzATP. **C**, BzATP-activated currents were recorded in Na^+ EC solution with low divalent cations and **D**, currents were recorded in Na^+ EC solution containing 1.58 mM Ca^{2+} and in response to 200 μM MgATP.

Fig. 6.

Inhibition of $P2X_{4/7}$ receptor currents by TNP-ATP and Brilliant Blue G (BBG). **A**, whole cell currents recorded in Na^+ EC solution, with and without pre-incubation with 2 μM TNP-ATP for 8 minutes. V_h=-30 mM. Histogram shows the peak current amplitudes (mean ± S.E.M., n > 10). **B**, representative currents recorded from HEK293 cells expressing either $P2X_7$, or with $P2X_4$ S341W EGFP in response to 30 μM BzATP in Na^+ ES solution with low divalent. BBG (1 μM) was applied for 10 minutes. V_h=-30 mM. Histogram shows mean current densities ± S.E.M. The data for $P2X_4$ was obtained using 30 μM MgATP (n > 4) instead of BzATP.

Fig. 1

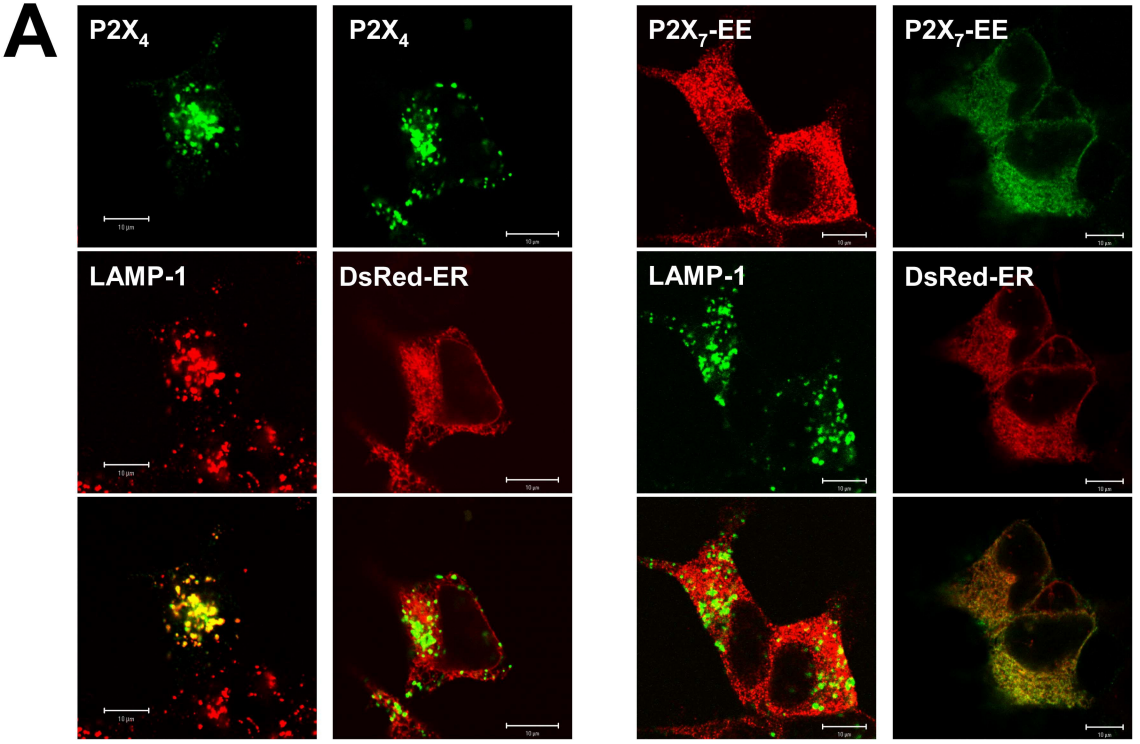
A
P2X4
P2X4
P2X7-EE
P2X7-EE
LAMP-1
DsRed-ER
LAMP-1
DsRed-ER

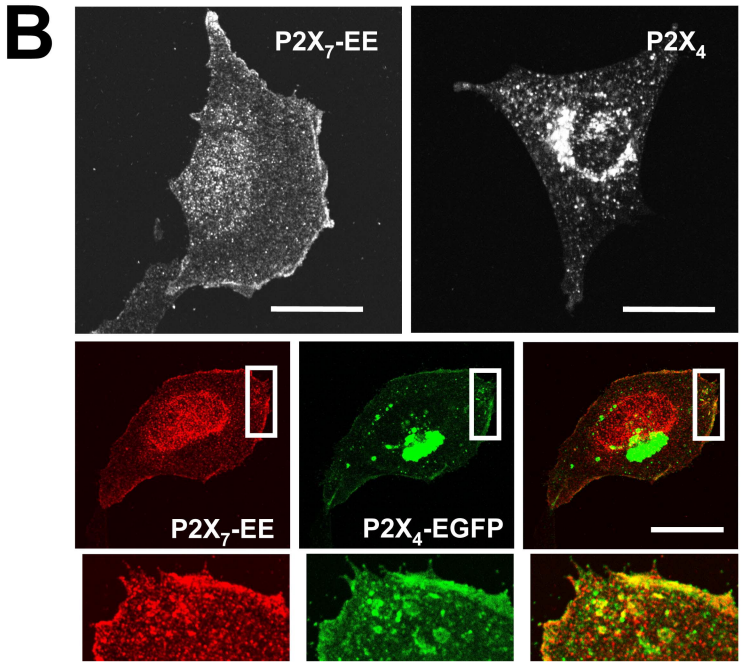
B
P2X7-EE
P2X4
P2X7-EE
P2X4-EGFP

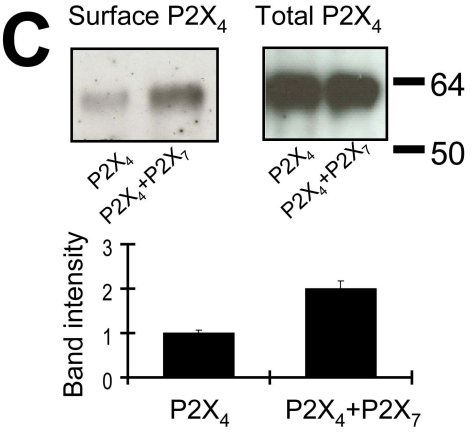
C
Surface P2X4
Total P2X4
64
50
P2X4
P2X4+P2X7
P2X4
P2X4+P2X7
Band intensity
3
2
1
0
P2X4
P2X4+P2X7

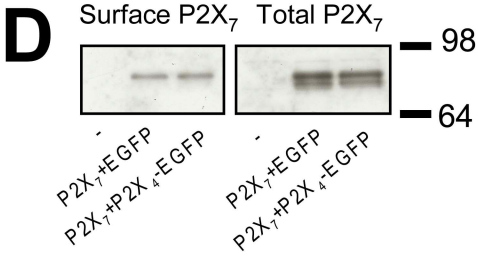
D
Surface P2X7
Total P2X7
98
64
-
P2X7+EGFP
P2X7+P2X4-EGFP
-
P2X7+EGFP
P2X7+P2X4-EGFP

Fig. 2

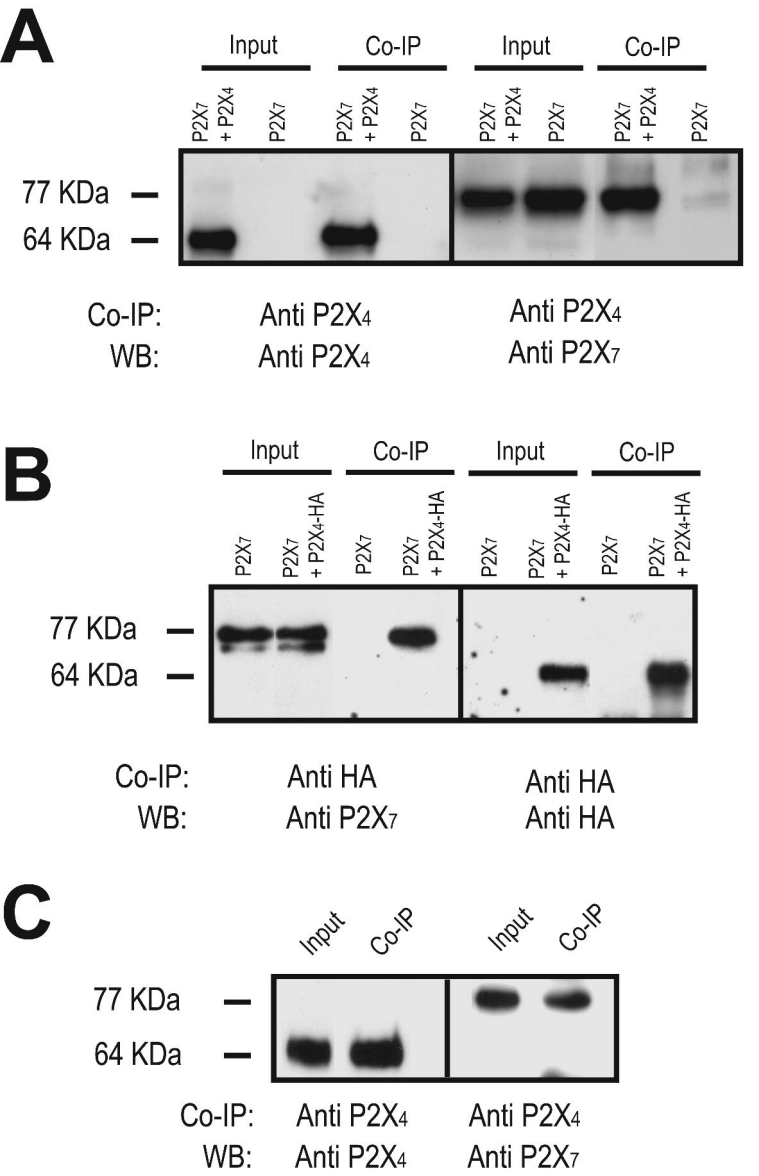
A
Input
Co-IP
Input
Co-IP
P2X7 + P2X4
P2X7
P2X7 + P2X4
P2X7
P2X7 + P2X4
P2X7
P2X7 + P2X4
P2X7
77 KDa
64 KDa
Co-IP: Anti P2X4
WB: Anti P2X4
Anti P2X4
Anti P2X7
B
Input
Co-IP
Input
Co-IP
P2X7
P2X7 + P2X4-HA
P2X7
P2X7 + P2X4-HA
P2X7
P2X7 + P2X4-HA
P2X7
P2X7 + P2X4-HA
77 KDa
64 KDa
Co-IP: Anti HA
WB: Anti P2X7
Anti HA
Anti HA
C
Input
Co-IP
Input
Co-IP
77 KDa
64 KDa
Co-IP: Anti P2X4
WB: Anti P2X4
Anti P2X4
Anti P2X7

Fig. 3

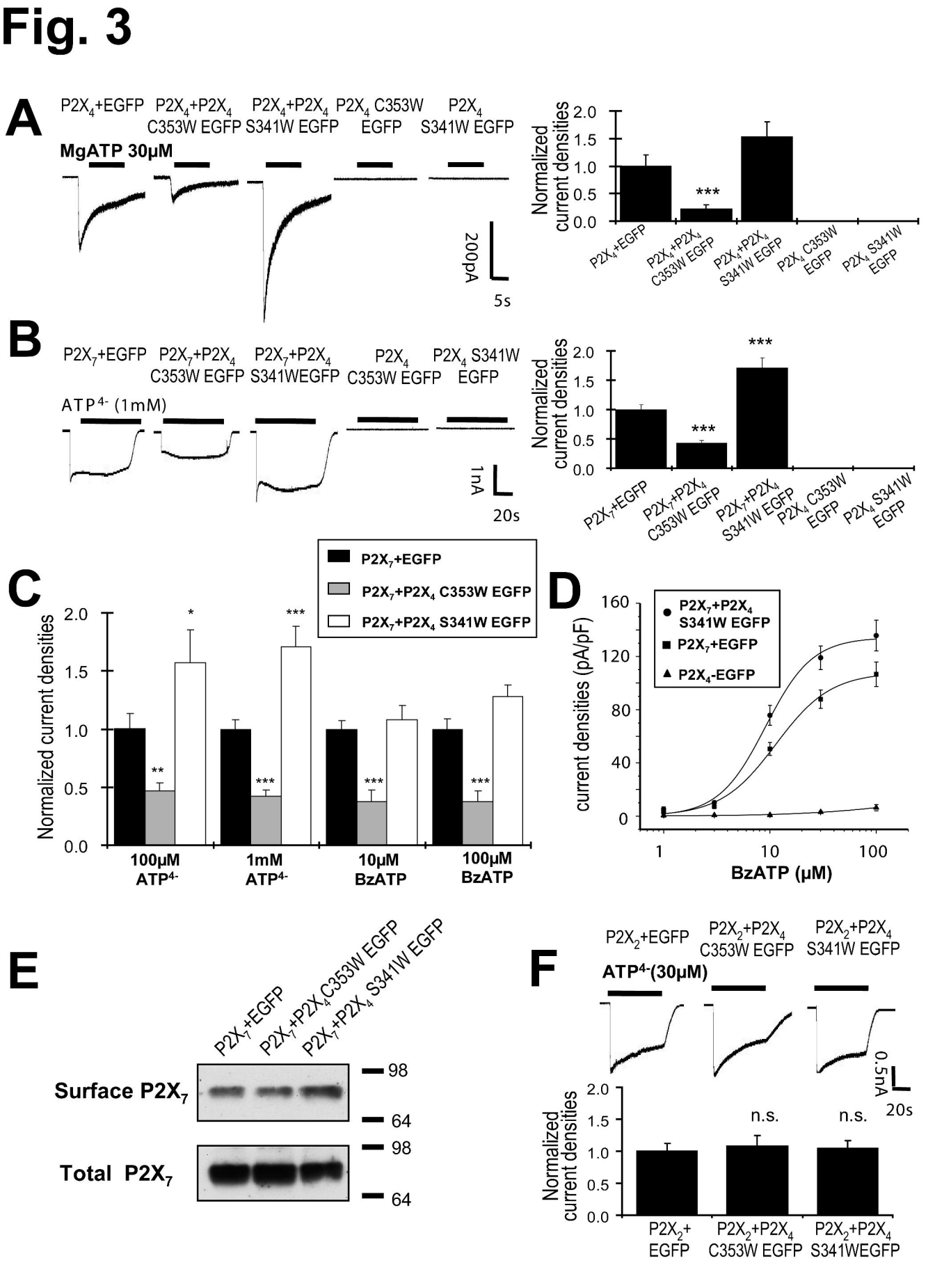
A
P2X4+EGFP
P2X4+P2X4 C353W EGFP
P2X4+P2X4 S341W EGFP
P2X4 C353W EGFP
P2X4 S341W EGFP
MgATP 30μM
200pA
5s
Normalized current densities
***
B
P2X7+EGFP
P2X7+P2X4 C353W EGFP
P2X7+P2X4 S341WEGFP
P2X4 C353W EGFP
P2X4 S341W EGFP
ATP4- (1mM)
1nA
20s
C
P2X7+EGFP
P2X7+P2X4 C353W EGFP
P2X7+P2X4 S341W EGFP
Normalized current densities
100μM ATP4-
1mM ATP4-
10μM BzATP
100μM BzATP
D
P2X7+P2X4 S341W EGFP
P2X7+EGFP
P2X4-EGFP
current densities (pA/pF)
BzATP (μM)
E
P2X7+EGFP
P2X7+P2X4 C353W EGFP
P2X7+P2X4 S341W EGFP
Surface P2X7
Total P2X7
98
64
F
P2X2+EGFP
P2X2+P2X4 C353W EGFP
P2X2+P2X4 S341W EGFP
ATP4-(30μM)
0.5nA
20s
n.s.
Normalized current densities
P2X2+ EGFP
P2X2+P2X4 C353W EGFP
P2X2+P2X4 S341WEGFP

Fig. 4

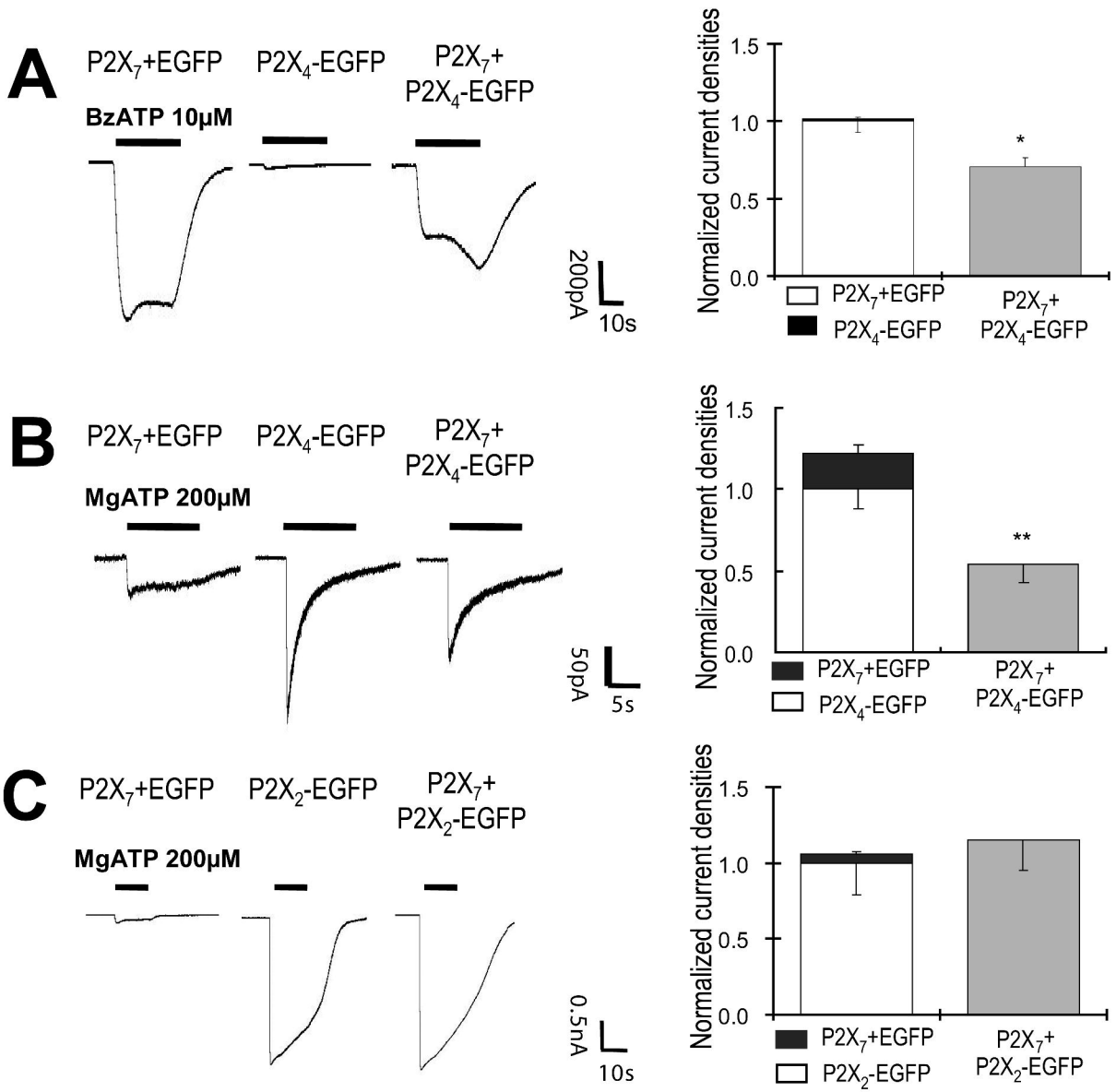
A
P2X7+EGFP
P2X4-EGFP
P2X7+ P2X4-EGFP
BzATP 10μM
200pA
10s
Normalized current densities
1.5
1.0
0.5
0.0
*
P2X7+EGFP
P2X4-EGFP
P2X7+ P2X4-EGFP
B
P2X7+EGFP
P2X4-EGFP
P2X7+ P2X4-EGFP
MgATP 200μM
50pA
5s
Normalized current densities
1.5
1.0
0.5
0.0
**
P2X7+EGFP
P2X4-EGFP
P2X7+ P2X4-EGFP
C
P2X7+EGFP
P2X2-EGFP
P2X7+ P2X2-EGFP
MgATP 200μM
0.5nA
10s
Normalized current densities
1.5
1.0
0.5
0.0
P2X7+EGFP
P2X2-EGFP
P2X7+ P2X2-EGFP

Fig. 5

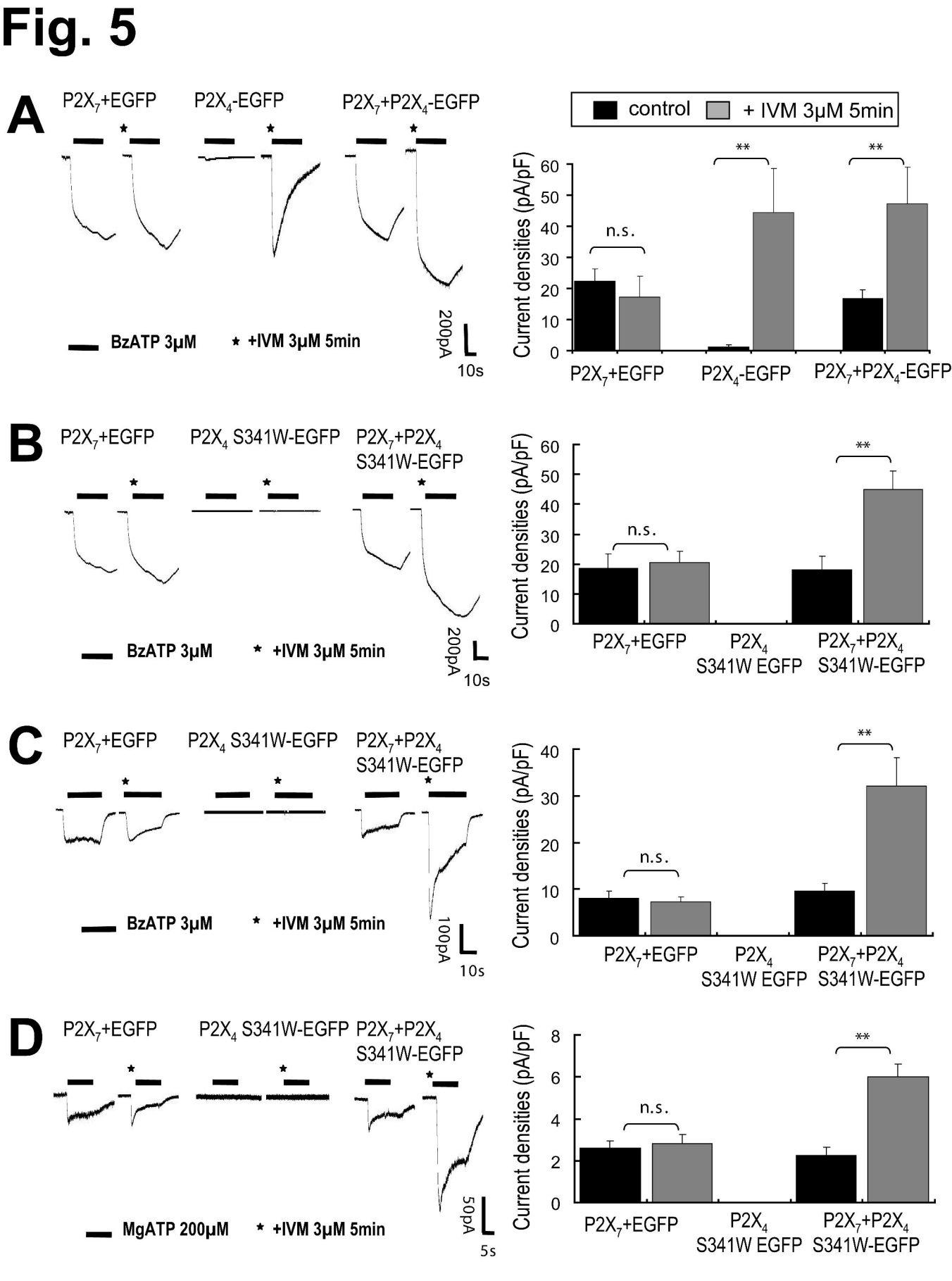
A
P2X7+EGFP
P2X4-EGFP
P2X7+P2X4-EGFP
BzATP 3μM
+IVM 3μM 5min
200pA
10s
control
+ IVM 3μM 5min
Current densities (pA/pF)
n.s.
**
P2X7+EGFP
P2X4-EGFP
P2X7+P2X4-EGFP
B
P2X7+EGFP
P2X4 S341W-EGFP
P2X7+P2X4 S341W-EGFP
BzATP 3μM
+IVM 3μM 5min
200pA
10s
P2X4 S341W EGFP
C
P2X7+EGFP
P2X4 S341W-EGFP
P2X7+P2X4 S341W-EGFP
BzATP 3μM
+IVM 3μM 5min
100pA
10s
D
P2X7+EGFP
P2X4 S341W-EGFP
P2X7+P2X4 S341W-EGFP
MgATP 200μM
+IVM 3μM 5min
50pA
5s

Fig. 6

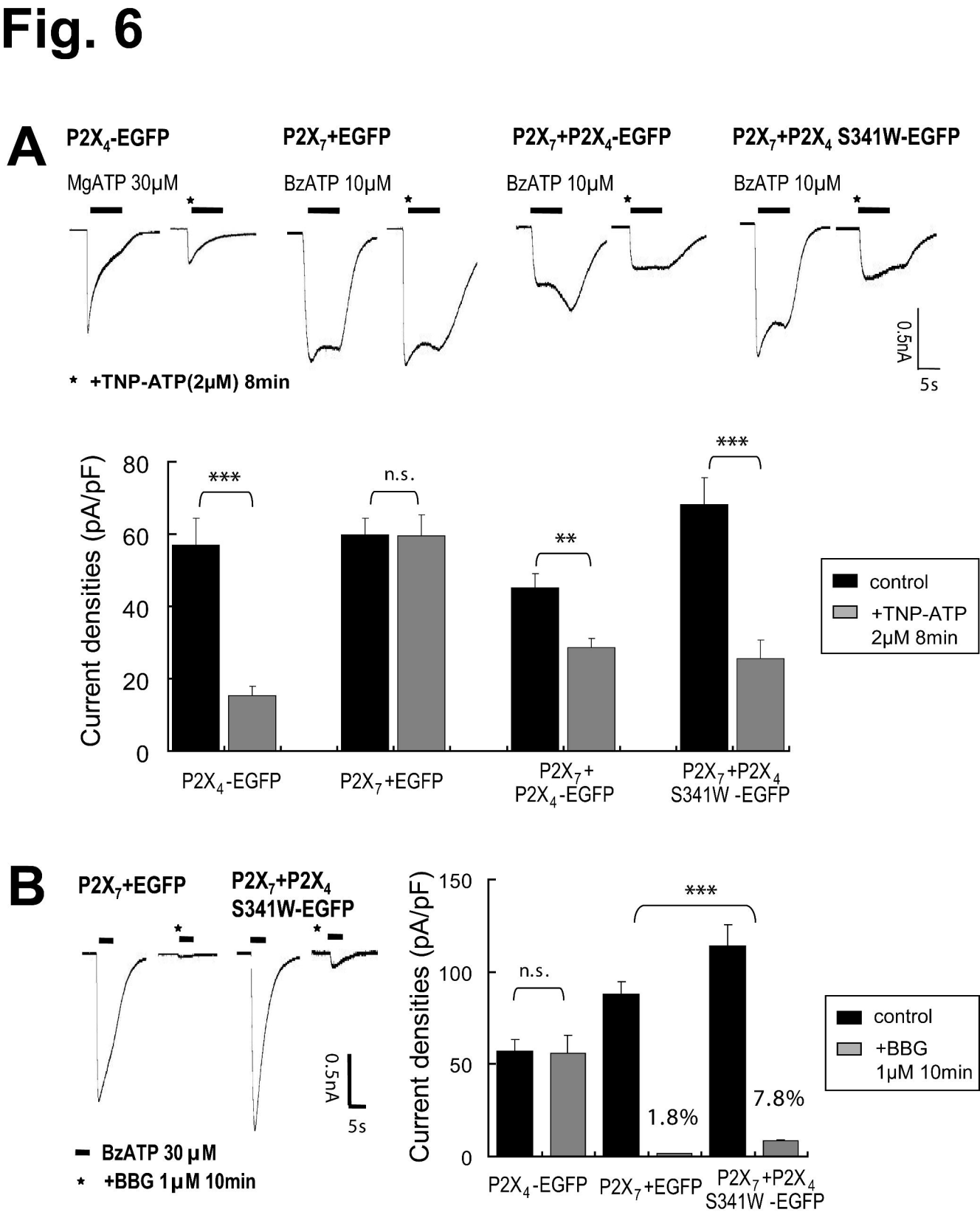
A
P2X4-EGFP
P2X7+EGFP
P2X7+P2X4-EGFP
P2X7+P2X4 S341W-EGFP
MgATP 30μM
BzATP 10μM
BzATP 10μM
BzATP 10μM
0.5nA
5s
* +TNP-ATP(2μM) 8min
Current densities (pA/pF)
80
60
40
20
0
***
n.s.
**
***
P2X4-EGFP
P2X7+EGFP
P2X7+ P2X4-EGFP
P2X7+P2X4 S341W -EGFP
control
+TNP-ATP 2μM 8min
B
P2X7+EGFP
P2X7+P2X4 S341W-EGFP
0.5nA
5s
BzATP 30 μM
* +BBG 1μM 10min
Current densities (pA/pF)
150
100
50
0
n.s.
***
1.8%
7.8%
P2X4-EGFP
P2X7+EGFP
P2X7+P2X4 S341W -EGFP
control
+BBG 1μM 10min